55. W. S. Benninghoff and W. N. Bonner, *Man's Impact on the Antarctic Environment* (Scientific Committee on Antarctic Research, International Council of Scientific Unions, Scott Polar Research Institute, Cambridge, United Kingdom, 1985), p. 56.
56. V. Ahmadjian, in *Antarctic Ecology*, M. W. Holdgate, Ed. (Academic Press, New York, 1970), vol. 2, p. 801; E. D. Rudolph, in *Antarctic Soils and Soil Forming Processes*, J. C. F. Tedrow, Ed. (American Geophysical Union, Washington, DC, 1966), vol 8, p. 105.
57. F. S. Chapin III and G. R. Shaver, in *Physiological Ecology of North American Plant Communities*, B. F. Chabot and H. A. Mooney, Eds. (Chapman & Hall, New York, 1985), p. 16; L. C. Bliss, in *ibid.*, p. 41.
58. E. I. Friedman, *Science* **215**, 1045 (1982).
59. N. J. Horowitz, R. E. Cameron, J. S. Hubbard, *ibid.* **176**, 242 (1972).
60. B. L. Umminger, in *Adaptations Within Antarctic Ecosystems*, G. A. Llano, Ed. (Proceedings of the Third SCAR Symposium on Antarctic Biology, Smithsonian Institution, Washington, DC, 1977), p. 347.
61. J. C. Hureau, D. Petit, J. M. Fine, M. Marneux, *ibid.*, p. 459.
62. R. M. G. Wells, M. D. Ashby, S. J. Duncan, J. A. MacDonald, *J. Fish Biol.* **17**, 517 (1980).
63. A. M. Slicher and G. E. Pickford, *Physiol. Zool.* **41**, 293 (1968).
64. E. A. Hemmingsen and E. L. Douglas, in *Adaptations Within Antarctic Ecosystems*, G. A. Llano, Ed. (Smithsonian Institution, Washington, DC, 1977), p. 479.
65. A. L. DeVries, in *Polar Research to the Present and the Future*, M. A. McWhinnie, Ed. (Westview, Boulder, CO, 1978), p. 175; A. L. DeVries, *Comp. Biochem. Physiol.* **73A**, 627 (1982).
66. P. W. Hochachka and G. N. Somero, *Biochemical Adaptations* (Princeton Univ. Press, Princeton, NJ, 1984).
67. P. J. Darlington, *Zoogeography: The Geographical Distribution of Animals* (Wiley, New York, 1966), pp. 675.
68. L. C. Bliss, in *Tundra Ecosystems: A Comparative Analysis*, L. C. Bliss, O. W. Heal, J. J. Moore, Eds. (Cambridge Univ. Press, Cambridge, 1981), p. 813.
69. M. G. White, in *Adaptations Within Antarctic Ecosystems*, G. A. Llano, Ed. (Smithsonian Institution, Washington, DC, 1977), p. 197.
70. R. W. Risebrough and M. Carmigniani, in *Conservation Problems in Antarctica*, C. Parker, Ed. (Allen, Lawrence, KS, 1972), p. 63.
71. We wish to thank the following for their comments, suggestions, and critical reviews of various parts of the manuscript: J. W. Harvey, R. A. Helliwell and M. A. Pomerantz commented on the upper atmosphere; D. H. Harwood, J. H. Mercer, M. L. Prentice and P. N. Webb commented on Cenozoic paleoclimatic history; and W. S. Benninghoff, J. C. Halfpenny, V. Komárková, K. A. Salzberg, and C. W. Sullivan commented on biological adaptations.

Gas-Phase Polymerization: Ultraslow Chemistry

HOWARD REISS

The mechanism of formation of polymer molecules in the gas phase is difficult to study because the involatile polymers tend to condense out of that phase. However, new techniques, involving the use of cloud chambers, have enabled workers to use the nucleation of liquid drops in supersaturated monomer vapors to detect single polymer molecules and therefore to work with so few simultaneously growing polymers that aggregation and condensation are avoided. Chain polymerization in which the chain carriers are either radicals or ions can therefore be studied in the vapor. Furthermore, the ability to work with such small concentrations of growing polymeric radicals, for example, makes it possible to avoid encounters between them that lead to recombination and the formation of "dead" polymers that are incapable of further growth. Many aspects of gas-phase polymerization can be studied including, besides radical and ion chains, ring-opening polymerization, initiation, radiation-induced polymerization, and especially "ultraslow" chemistry.

CHAIN POLYMERIZATION IN THE CONDENSED PHASE (USUally liquid) has been studied extensively (*1*, chapters 3 through 6) and is of major importance to the polymer industry. The steps involved in a typical process are shown for the production of polystyrene from styrene ($\phi CH{=}CH_2$, where ϕ represents a phenyl group) via a free radical mechanism:

$$I \xrightarrow{k_d} 2R\cdot \qquad \text{(thermal or photoinitiation)}$$

$$R\cdot + \phi CH{=}CH_2 \xrightarrow{k_p} RCH_2{-}\dot{C}H \quad (\phi)$$

$$RCH_2\dot{C}H \quad (\phi) + \phi CH{=}CH_2 \xrightarrow{k_p}$$

$$RCH_2{-}CH_2{-}CH_2{-}\dot{C}H \quad (\phi,\ \phi) \qquad \text{(propagation)}$$

and so forth

$$R(CH_2CH)_n{-}CH_2\dot{C}H + R(CH_2CH)_m{-}CH_2\dot{C}H \quad (\phi,\ \phi,\ \phi,\ \phi)$$

$$\xrightarrow{k_t} R(CH_2CH)_{n+1}{-}(CHCH_2)_{m+1}R \quad (\phi,\ \phi) \qquad \text{(termination)}$$

Scheme 1

where k_d, k_p, and k_t are rate constants for dissociation, propagation, and termination, respectively; I is an initiator that can decompose thermally or photolytically; and R· is a free radical. Other elementary steps are possible [such as chain transfer (*1*)], in which both a "dead" polymer and a monomeric radical that can still propagate are formed. A separate initiator may not be necessary with photochemical initiation. Termination not only leads to smaller polymers but also complicates both theory and measurement. In liquids it can be forestalled by the use of emulsion polymerization (*1*), and recently by the use of plasma-induced polymerization (*2*). Propagation that involves ion chains is also possible.

The author is in the Department of Chemistry and Biochemistry, University of California, Los Angeles, CA 90024.

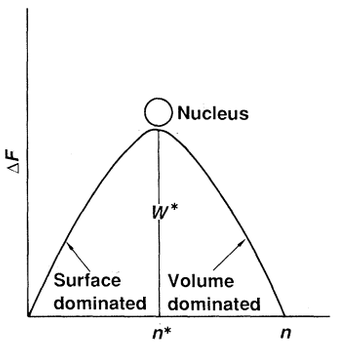

Fig. 1. Qualitative illustration of the nucleation free energy barrier.

The polymerization rate is usually defined as the average rate of disappearance of the monomer or as the rate of increase of the average molecular weight (*3*). The growing free radicals are themselves present in low concentrations ($\sim 10^{-8} M$), and little attempt has been made to observe them directly. Thus it is not the rate of accumulation of polymers of a given size that is measured; only an average for all sizes is measured. For smaller polymers, k_p may depend on size, but it is difficult to control the processes in scheme I so that this effect can be measured.

In order to study the polymer process in scheme 1 without interference from termination it is necessary to run the reaction under conditions with so few simultaneous radical chains present that two chains cannot meet and recombine. It would also be useful to be able to measure the rate of production of radicals of one particular size (rather than of an average size), especially a small size, but, with conventional means and at such low concentrations, there are serious problems of detection. Some of these problems have been solved by a new method that is applicable to gas-phase polymerization and in which the polymers act as centers for the nucleation of liquid drops. "Ultraslow" reactions with initiation rates less than one free radical per cubic centimeter per second have been observed when this method is applied. Furthermore, other elementary polymer processes that cannot be observed by conventional means can be accessed by this method.

Although there have been many papers published about "gas-phase polymerization," most of these concern heterogeneous processes in which the monomer resides in the vapor while the polymer grows on the walls of the reaction vessel. A number of workers have made successful (or partially successful) attempts to study true homogeneous gas-phase polymerization (*4*). The tendency for the involatile polymer to condense out of the vapor either limited these studies to small polymers (dimers, trimers, and so forth) or required the studies to be conducted in the presence of aerosol. The avoidance of condensation, like recombinative termination, allows only a few chains to grow simultaneously, and again raises the problem of detection.

Nucleation and Cloud Chambers

An extensive literature on the subject of nucleation is available (*5*). The theory is difficult, and only recently have rigorous approaches been attempted (*6*). The phenomenon is only sketched here, and discussion is limited to the condensation of supersaturated vapors. Consider a simple, one-component vapor (water vapor), for example, supersaturated so that its relative humidity (RH) exceeds 100%. Attainment of stable equilibrium in this system depends on a "reaction" in which individual vapor molecules aggregate to form clusters (essentially van der Waals molecules) and finally larger fragments of liquid. In the simplest case, the cluster is treated as a liquid drop. The free energy change ΔF involved in the clustering process consists of two parts, (i) ΔF_{bulk}, which is associated with the formation of the volume of the cluster and represents a free energy decrease because the vapor is supersaturated, and (ii) $\Delta F_{surface}$, which accompanies the formation of the interface between cluster and vapor, and represents a free energy increase proportional to the cluster surface area. With smaller clusters, the positive $\Delta F_{surface}$ dominates so that ΔF increases with size. However, with increasing size the negative ΔF_{bulk} overcomes this effect so that ΔF passes through a maximum. The result is the free energy barrier illustrated qualitatively in Fig. 1, where ΔF is plotted versus n, the number of molecules in the cluster. At the maximum, n is denoted by n^*, and the height of the barrier W^* is given by

$$W^* = (16/3)\pi\sigma^3 v^2 (k_B T \ln S)^{-2} \quad (1)$$

where σ is the surface tension, v is the volume per molecule in the liquid, k_B is the Boltzmann constant, T is the temperature, and the supersaturation $S = P/P_e$ where P is the actual pressure in the vapor and P_e is the equilibrium vapor pressure at the temperature T. The relative humidity is obtained by multiplying S by a factor of 100.

The cluster (drop) of size n^* is called a "condensation nucleus." Once formed, it can grow spontaneously (with a decrease in free energy) into a macroscopic liquid drop. The value of n^* depends on S and is typically small (between 10 and 1000). The nucleation rate (rate of drop formation) is that rate at which clusters of nucleus size form. This process involves a sequence of reversible "reactions" in which the cluster adds molecules one at a time. For the rate of nucleation J, analysis yields

$$J = Ae^{-W^*/k_B T} \quad (2)$$

in which the preexponential factor A is only weakly dependent on supersaturation. From its position in Eq. 2 it is clear that W^* is the free energy of activation for the process.

From a calculation of J as a function of S from Eq. 2 for water vapor at 300 K and at 120% RH or a supersaturation of 1.2, an average of 10^{996} seconds will pass before the appearance of a single drop in a cubic centimeter of vapor. This is a meaninglessly long time, yet water condensation occurs readily at much lower relative humidities because preexisting surfaces such as dust particles and walls catalyze condensation by means of heterogeneous nucleation. The uncatalyzed process to which Eq. 1 refers is termed homogeneous nucleation. At 280% RH or $S = 2.8$ the same calculation shows that about 10^6 seconds will pass before a drop forms, but that for $S = 3.11$ only 1 second is required while for $S = 3.4$, 10^{-4} second is enough. Thus at 300 K, for the homogeneous nucleation of water vapor to occur at a sensible rate, for example, at 1.0 drop cm^{-3} sec^{-1}, RH values in excess of 300% are required; J remains negligible until a "critical supersaturation" S_c is reached, at which point the value of J increases explosively.

This extreme critical behavior may be understood on physical grounds. The free energy barrier constitutes a "dam" over which the flow of clusters (in size space) is so constrained that those behind the dam (including the nucleus) fall into quasiequilibrium with one another, such that the concentration of nuclei c^* is mandated by the law of mass action to depend on S according to the relation $c^* = K_e S^{n^*}$, where K_e is an equilibrium constant. If n^* is of the order of 100, a slight change in S can lead to an enormous change in c^* and consequently in the rate of nucleation.

Measurements of S_c for homogeneous nucleation can be made in a "cloud chamber," of which two types are particularly important, (i) the upward diffusion cloud chamber and (ii) the expansion (Wilson) cloud chamber. The diffusion chamber was pioneered by Franck and Hertz (*7*) and developed to a high degree of perfection by Katz and co-workers (*8–11*) (Fig. 2A). It consists of two circular metal plates separated by a glass cylinder. The lower plate is heated

and the upper one cooled. The liquid, within whose vapor S_c is to be determined, forms a shallow pool on the heated lower plate. The space above the liquid is filled with helium. The liquid evaporates, diffuses through the helium to the upper plate, condenses to a smooth film, and drains back to the pool along the glass so that a constant state of reflux is established. The various transport processes combine to produce the steady vertical distribution of supersaturation (Fig. 2B).

How does one measure S_c in this chamber? The temperatures of the two plates are adjusted, and the curve of S versus elevation (or temperature) develops until drops that are formed near the "peak" of the curve are observed by scattered light to fall through a laser beam at a rate of about 1 sec^{-1}. The peak of the S curve is then rotated 90° and mapped onto the space of Fig. 3, in this case for nonane (*9*), where many peaks that correspond to similar experiments performed with different pairs of plate temperatures are plotted. The "envelope" of these peaks (not shown) constitutes the measured curve of S_c versus T. The dashed curve predicted by theory (Fig. 3) is calculated with Eq. 2 by setting $J^* = 1.0$ cm^{-3} sec^{-1} and solving for S_c. Agreement between theory and experiment is within a few percent. Such agreement is typical for a large variety of substances, including water (*12*), the alcohols (*8, 13*), the *n*-alkanes (*9*), benzene, toluene, butylbenzene, *o*-xylene (*10*), menthol (*14*), stearic acid (*15*), the halogenated hydrocarbons (*9*), and vinyl acetate (*16*).

In the expansion cloud chamber, the vapor is contained in a space filled with a supporting gas (for example, argon) above the liquid, which rests on a piston (*17*). The piston can be lowered in rapid expansion, during which time the adiabatically cooled vapor becomes supersaturated to a degree calculable from the adiabatic law. Drops first appear when the supersaturation equals S_c. Schmitt (*17*) discusses perhaps the most precise expansion chamber available at the present time.

The theory of nucleation can be extended to binary and multicomponent systems (*18, 19*) such as a vapor mixture of water and sulfuric acid. The free energy of cluster formation for binaries depends on the cluster's molecular contents of both species, so that the simple "barrier" exhibited in Fig. 1 becomes a surface on which the nucleus corresponds to a saddle point (*18*).

The foregoing discussion applies to homogeneous nucleation for a monomer vapor, and the agreement between theory and experiment for a polymerizable monomer (for example, vinyl acetate) is no different than for nonpolymerizable species. Suppose, however, that a single polymer formed of the same monomer is inserted into the monomer vapor. The polymer can then begin to aggregate (reversibly) with monomers, so that a binary cluster of nucleus size is eventually created, followed by the appearance of a macroscopic liquid drop. Theory allows the estimation of the average time τ that elapses after the insertion of the polymer and before a nucleus is formed (*20*). For styrene vapor at 247.6 K and $S = 11.42$ (far below $S_c \approx 30$ for styrene at this temperature so that homogeneous nucleation does not occur) it can be shown that, if the polymer has a DP (degree of polymerization or number of monomer units in the polymer) of 8, $\tau = 1.2 \times 10^7$ seconds. With DP = 9, $\tau = 6.2 \times 10^2$ seconds, while with DP = 10, $\tau = 3.1 \times 10^{-2}$ second, and with DP = 11, $\tau = 1.6 \times 10^{-6}$ second. Thus an increase in DP of only 37% is accompanied by a decrease in τ of 13 orders of magnitude. A meaningful laboratory time (1 second) occurs between DP = 9 and 10, where, for only an 11% increase in DP, τ decreases by four orders of magnitude.

Now suppose that a polymer is grown in the supersaturated monomer vapor via the chain process of scheme 1. The growing polymer will in effect never nucleate a drop at DP = 8 but will do so almost instantaneously at DP = 11. Thus the presence of the polymer of DP = 11 can be detected by the drop it produces, so that one can "tune" to a given size (the "tuneable" size) by controlling the supersaturation.

Why is the polymer so effective in nucleating a drop, and why is the process so critical? The following is an inexact, but essentially correct, explanation (*20*). The barrier in Fig. 1 is generally high, so that the exponent in Eq. 2 is large. To a first approximation, a polymer with DP = n resembles a cluster of size $n \leq n^*$. The ascent of the barrier required to form a nucleus need then begin not at the bottom but at a substantial elevation corresponding to n = DP. The height is thus effectively reduced, and with it the exponent in Eq. 2. However, even a small reduction in the large exponent amounts to an enormous increase in nucleation rate, and this explains the remarkable variation in τ discussed above.

Although the polymer eventually forms a nucleus, at which point it may be regarded as dissolved in a drop of its own monomer, it is mostly bare during its growth, so that growth really occurs in the vapor. This situation is related to the fact that when drops are nucleated at a rate of about 1.0 cm^{-3} sec^{-1}, during 1 second in 1 cm^3 of vapor, on the average, a nucleus will be present only during an accumulated period of 10^{-11} second (*21*).

The diffusion cloud chamber is inexpensive and simple, but, because it generates gradients of both temperature and monomer pressure, it does not offer high precision with respect to the measurement of polymer kinetics. In contrast, the expansion chamber provides a uniform vapor environment within which polymers may grow. However, upon expansion to a given degree of supersaturation, all polymers larger than the tuneable size form drops. Thus by varying S, and therefore the tuneable size, the cumulative yield for polymers greater than the tuneable size is measured.

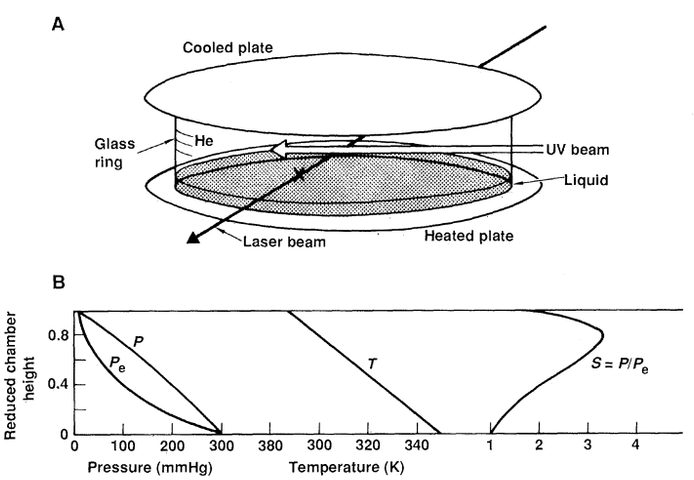

Fig. 2. (**A**) Sketch of diffusion cloud chamber with relevant components indicated. The optically defined volume of observation in the laser beam through which drops fall is marked by **X**. (**B**) Typical courses of diffusant partial pressure P, saturation pressure P_e, temperature T, and supersaturation S in diffusion cloud chamber. [Reprinted from (*36*) with permission, copyright from *The Journal of Chemical Physics*]

Chemistry and Cloud Chambers

The cloud chamber was developed as a tool for physicists. Eventually its major application was to reveal high-energy particle tracks. Its application to chemistry represents an evolution similar to that of the molecular beam—also originally a tool for physicists. In 1939, Crane and Halpern (*22*) tried (unsuccessfully) to induce nucleation with small, single neutral molecules. In 1969, Allard and Kassner (*23*) suggested that individual molecules of H_2O_2 could nucleate water vapor, an idea that eventually was discarded. Although single nonpolymeric molecules are ineffective, small concen-

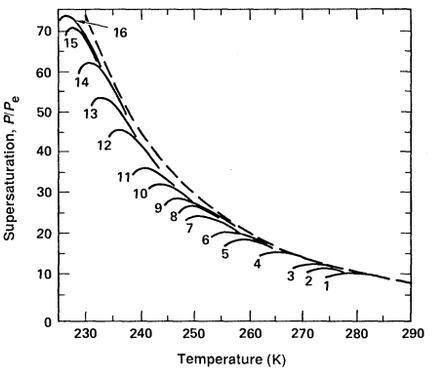

Fig. 3. Critical supersaturation versus temperature for nonane (*8*); helium carrier gas; diameter-to-height ratio 5.99:1. Dashed line represents theory. The envelope of the various peaks is the experimental curve. [Reprinted from (*36*) with permission, copyright from *The Journal of Chemical Physics*]

trations of them [$\sim 10^6$ cm^{-3} (*24*), as in the case of H_2SO_4 in water vapor] can cause the formation of a binary nucleus. The kinetics of the ultraslow photooxidation of SO_2 in the presence of water vapor was successfully investigated in real time with the use of nucleation for detection (*25*). Other chemical kinetic studies have also been attempted (*26*). Katz and co-workers (*27*) were the first to adapt nucleation to microanalysis. Typically, a supersaturated vapor doped with an impurity in the parts per trillion to parts per million range in a diffusion cloud chamber is irradiated with ultraviolet (UV) light. An involatile photochemical product generated from the impurity induces nucleation. For identification, the dependence of nucleation rate on wavelength is matched to the wavelength dependence of the extinction coefficient times the quantum yield (*28*).

Studies of Chain Polymerization

Figure 2 shows how the kinetics of polymerization may be investigated in a diffusion cloud chamber with monomer liquid on the lower plate. In one approach (*29*), a UV beam enters the monomer vapor at the level of maximum supersaturation. Radicals form in the beam and grow and diffuse until they are lost to the chamber walls. If the beam is steady, a steady state of polymer sizes is established up to but not exceeding DPs of the "tuneable size." Radicals of this size are removed from the distribution by forming drops that fall through the laser beam to be counted. A low photon flux is used so that few enough polymer radicals grow simultaneously to avoid recombination and condensation. The observed rate of nucleation then equals the rate of production of polymers of the tuneable size.

If the light intensity is increased sufficiently, the nucleation rate is reduced because of recombination, an effect used as a diagnostic to indicate nucleation due to polymers (*29*). Methods need to be and have been developed (*29*) to ascertain that each nucleus contains only one polymer. The presence of more than one polymer molecule makes it very difficult to compare the experiment with theory.

Nonsteady experiments (*20, 30, 31*) are more useful than steady ones, in that the tuneable size is measured rather than estimated from an imperfect nucleation theory. A brief pulse of UV photons is used, a fraction of which creates radicals that grow into polymers. The number of polymers of tuneable size x at time t after the pulse is (*20, 32*)

$$N_x = N_0 e^{-k_p M t}\,[(k_p M t)^{x-1}/(x-1)!] \qquad (3)$$

where N_0 is the initial number of free radicals and M is the monomer concentration. Since x is fixed, the nucleation rate is given by $J = k_p M N_{x-1}$. Figure 4 is a plot of J versus t for a pulse experiment on vinyl acetate (*31*). The curve is a least-squares fit of Eq. 3 to these points; from it x and k_p can be determined.

Even after averaging over 400 runs, the data are still "noisy," which is a result of the ultraslow rate being measured; the maximum rate of product molecule formation in Fig. 4 is 0.6 cm^{-3} sec^{-1}. From the measured "noise," N_0 can be determined (*20*), because noise increases as N_0 decreases. Thus the quantum yield can be measured and the system can be used as its own actinometer.

Styrene in the liquid phase is known to produce its own free radicals (initiation rate, $I < 10^{10}$ cm^{-3} sec^{-1}) at room temperature (*1*). Attempts to demonstrate this thermally self-initiated process by conventional means in the vapor phase have been inconclusive; the pressure of styrene vapor does not seem to decrease with time for temperatures up to 400°C (*33*). Self-initiation is still not fully understood (*34*). In the liquid phase, the average molecular weight of the polymer decreases with increasing temperature, an effect attributed to increased recombination at higher initiation rates (*35*).

Figure 5 for styrene (*36*) is the counterpart of Fig. 3 for nonane. The envelope of the many peaks is the experimental curve of S_c versus T. Unlike previous studies, it lies far below theory (curve appearing in the figure) for homogeneous nucleation. That this discrepancy is not a feature of nonpolymerizable styrene-like molecules is demonstrated by a similar study (*36, 37*) for ethylbenzene (ϕCH_2CH_3, Fig. 6), in which theory and experiment are in agreement.

Figure 5 is explained as follows. The cloud chamber can be approximated as a cylindrical vessel of height $2L$ and radius a that contains styrene vapor in a uniform convectionless state. Radicals are initiated uniformly at rate I. Termination is absent, and the radicals grow into polymers which diffuse and are irreversibly lost to the walls. With r and z as cylindrical coordinates, the steady concentration of polymers (*20, 36, 37*) with DP = j is

$$N_j(z,r) = \sum_{\alpha} \sum_{m=0}^{\infty} \left[\frac{(-1)^m 4I}{D_1 L \alpha J_1(\alpha)\omega_m}\right] \times \left\{\frac{\prod_{i=1}^{j-1}(K_i/D_{i+1})}{\prod_{i=1}^{j}\left[\left(\frac{\alpha}{a}\right)^2 + \frac{K_i}{D_i} + \omega_m^2\right]}\right\} (\cos \omega_m z) J_0\left(\frac{\alpha}{a} r\right) \qquad (4)$$

in which $K_i = k_p^{(i)} M$, D_i is the diffusivity, J_0 and J_1 are Bessel functions, and α and ω_m are specified eigenvalues. The appearance of i in $k_p^{(i)}$ and D_i indicates that propagation and diffusion can depend on polymer size.

The discrepancy between theory and experiment in Fig. 5 can be explained (*20*) by the preestablishment of the distribution described by Eq. 4. At given values of T and S, a polymer of tuneable size may

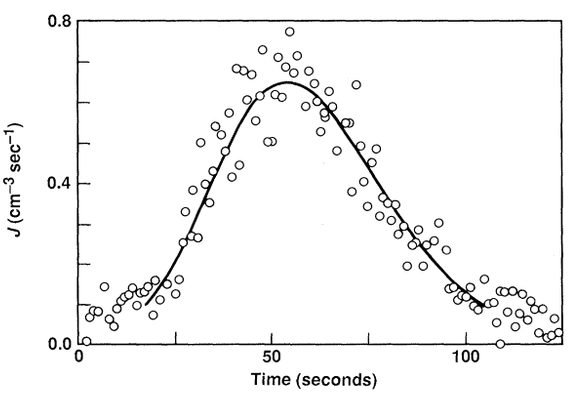

Fig. 4. Nonsteady-state nucleation in vinyl acetate after a UV pulse. Open circles are experimental points averaged over 400 runs. The curve is a least-squares fit to Eq. 4. [Reprinted from (*31*) with permission, copyright 1986 from D. Reidel Publishing Company, Dordrecht, Netherlands]

Fig. 5 (left). Critical supersaturation versus temperature for styrene. Solid line represents theory, envelope represents experiment. Note the large discrepancy. [Reprinted from (*36*) with permission, copyright from *The Journal of Chemical Physics*] **Fig. 6 (right).** Critical supersaturation versus temperature for ethylbenzene. Solid line represents theory, envelope represents experiment. [Reprinted from (*36*) with permission, copyright from *The Journal of Chemical Physics*]

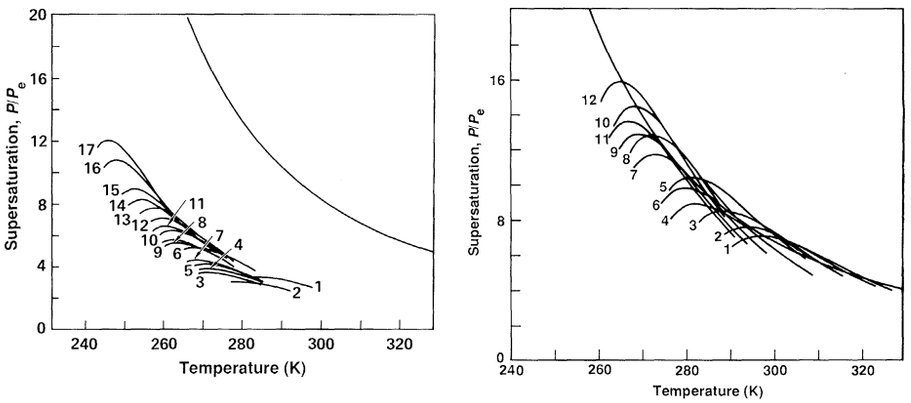

not exist in this distribution. As S is increased, the tuneable size is reduced into the distribution and removed in a drop. Before another drop can form, another "tuneable" polymer must be propagated. Thus the rate of drop formation is the rate of chemical propagation which can therefore be measured. This occurs below the value of S_c required for homogeneous nucleation, so that the envelope curve lies below the theoretical one.

Although a full discussion is not possible here (*36, 37*), the "envelope curve" in Fig. 5 can be raised toward the theoretical curve by the addition of a volatile "retarder" (phenylacetylene), and the envelope in Fig. 6 (for ethylbenzene) can be lowered below the theoretical curve by the addition of 5% styrene. The value of k_p in the vapor was measured; it was almost the same as that found in the liquid. The initiation rate I in the vapor was found to lie between 1.0 and 2×10^2 cm^{-3} sec^{-1}, and is likely to be second order in the monomer concentration. Schmitt (*38*), using the more precise expansion chamber, found I closer to the lower value of 1.0 radical per cubic centimeter per second. It is not surprising that, as time passes, a spontaneous reduction in pressure cannot be measured at room temperature in styrene vapor. For these values of I and k_p, it would require 5×10^8 years for such a decrease to occur. It is a measure of the sensitivity of the cloud chamber technique that it allows self-initiated polymers in the vapor to be detected immediately. The tuneable sizes in Fig. 5 were found to lie between DP = 9 and DP = 25, and at higher temperatures larger polymers were produced, in contrast to the situation in liquids. This tends to confirm the absence of termination. The total steady concentration of radicals (all sizes) was estimated to be on the order of 30 cm^{-3}, thus eliminating all possibility of recombination. For polymers such as vinyl acetate (not self-initiated), similar experiments were performed (*39*) by adding a trace of a thermally decomposable initiator (for example, benzoyl peroxide) to the vapor. Such experiments can clarify the ultraslow initiation process.

Another experiment that cannot be performed by conventional means involves the copolymerization of monomers A and B to form block copolymers of the type ABAAAABBBAAABBBBA. Such a sequence implies that an A end unit prefers to add an A, but not exclusively, and vice versa. For ordinary copolymerization this situation is rare (*1*, p. 376). Usually, either both types of end unit prefer to add only one of the monomers or both are indiscriminate. However, if the rare alternative is assumed, although the distribution of compositions among large polymers, say, with respect to A, will be unimodal about some average, the compositions of small polymers (because of the predilection against "switching") will consist more exclusively of blocks of either A or B. Thus the distribution of compositions is likely to be bimodal (*40*) around compositions of pure A or B. Isoprene [CH_2=C(CH_3)–CH=CH_2] contains two double bonds, and can polymerize to form chains with several kinds of repeat units (*1*, section 3-14) and thus effectively forms a copolymer.

Figure 7 is for a signal-averaged pulse experiment (*41*) with isoprene vapor (similar to that for vinyl acetate in Fig. 4). Small tuneable sizes are involved (different for different compositions), and the two peaks that occur at separate times may reflect the "bimodal" rates at which polymers of these sizes are produced. It would be quite difficult to observe this bimodal distribution by conventional means.

State of the Art and Future Studies

The preceding account has necessarily been descriptive and limited to a few examples. However, this field is new, and most of the work has been aimed at the demonstration of feasibility and at the study of the most simple systems. The accuracy of measurement has not been high; and errors of only 20% (sometimes 100%) have been considered good. Among the problems to be investigated are the study of ion chains, ring-opening polymerization (*1*, chapter 7), organometallic initiators (*42*), and gas-phase radiation-induced polymerization. Ion propagation by means of free ions can be orders of magnitude faster than free radical propagation (*43*). Extremely slow initiators, some of them involving inorganic reactions, can be studied as long as propagation is sufficiently fast. Polymerization then becomes of secondary interest and is itself used as an amplifier for the study of the ultraslow chemistry involved in the initiating step. The possibilities for radiation-induced polymerization are

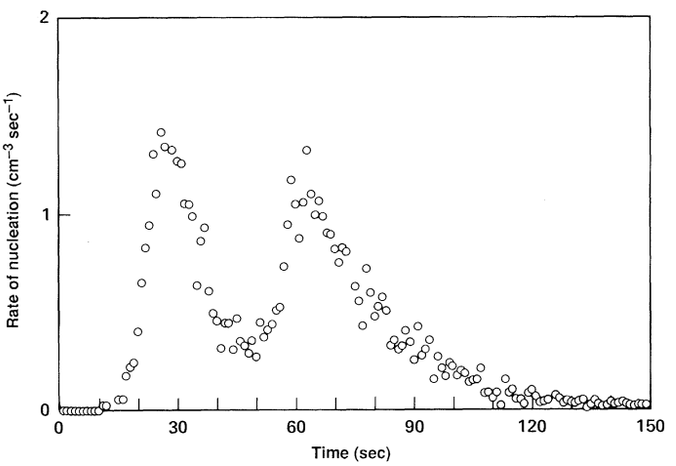

Fig. 7. Nonsteady nucleation in isoprene after a UV pulse. Open circles are points signal-averaged over 200 runs. The existence of two maxima is possibly a result of the bimodal distribution of compositions.

particularly exciting. For example, a beta particle will produce a track in which the excited particles are both ions and free radicals (*44*). The ions are subject to geminate recombination (*45*), but ion propagation can be so fast that significant polymerization can still occur [especially in superdry media (*46*)]. Of course, the radicals in the track may also propagate, although in the case of ethyl vinyl ether it now appears that propagation is exclusively ionic (*46*).

The cloud chamber technique offers the possibility of directly observing free radical, cationic, and anionic chains, and of distinguishing between them. To understand how this could be accomplished, consider a monomer vapor in an expansion cloud chamber. The vapor may be doped with a suitably small trace of phosphine that contains the beta-emitting phosphorus isotope. Very sparse beta tracks will be produced. These can be "developed" by conducting an adiabatic expansion and forming drops on the polymers grown from the ions and radicals in the track. Furthermore, the ion and radical chains could be separated (before expansion) by the application of an electric field. Thus, one could ascertain that both radical and ionic chains were involved. Whether the ions were cations or anions or both could be established from the direction of displacement of the track. In a sense, when such experiments are performed, the circle will have been completed; the cloud chamber will once again be used for the observation of tracks, except that now the drops will have been nucleated by polymers rather than ions.

REFERENCES AND NOTES

1. G. Odian, *Principles of Polymerization* (McGraw-Hill, New York, 1970).
2. C. I. Simionescu and B. C. Simionescu, *Pure Appl. Chem.* **56**, 427 (1984); B. C. Simionescu, *Polym. Bull. (Berlin)* **6**, 415 (1982).
3. F. C. Goodrich and M. Cantow, *J. Polym. Sci. Part C* **8**, 269 (1965); G. R. Alms, G. R. Patterson, J. R. Stevens, *J. Chem. Phys.* **70**, 2145 (1979).
4. H. W. Melville, *Proc. R. Soc. London Ser. A* **163**, 511 (1937); *ibid.* **167**, 99 (1938); G. Gee, *Trans. Faraday Soc.* **34**, 712 (1938); J. W. Breitenbach, *Oesterr. Chem. Z.* **42**, 232 (1939); D. H. Volman, *J. Chem. Phys.* **14**, 467 (1946); H. W. Melville and R. F. Tuckett, *J. Chem. Soc. Faraday Trans. 2* (1947), pp. 1201 and 1211; J. Heicklen, *J. Am. Chem. Soc.* **87**, 445 (1965); D. G. Marsh and J. Heicklen, *ibid.* **88**, 269 (1966).
5. M. Volmer, *Kinetic der Phasenbildung* (Steinkopf, Dresden, 1939) (translated into English by the Intelligence Department, Air Materiel Command, U.S. Air Force, as document ATI No. 81935); J. Frenkel, *Kinetic Theory of Liquids* (Oxford Univ. Press, New York, 1946), chap. 7; *J. Chem. Phys. 1* (1939), pp. 200 and 538; F. F. Abraham, *Homogeneous Nucleation Theory* (Academic Press, New York, 1974); A. C. Zettlemoyer, *Nucleation* (Dekker, New York, 1969); A. C. Zettlemoyer, Ed., *Nucleation Phenomena* (Elsevier Scientific, New York, 1977); H. Reiss, *Ind. Eng. Chem.* **44**, 1284 (1952); "Precipitation" [*Faraday Disc. Chem. Soc.* **61** (1976)]; J. P. Hirth and G. M. Pound, in *Progress in Materials Science*, B. Chalmers, Ed. (Pergamon, London, 1963), vol. 11; R. Becker and W. Döring, *Ann. Phys.* **24**, 719 (1935); J. B. Zeldovich, *Acta Physicochem. USSR* **18**, 1 (1943).
6. K. Binder and D. Stauffer, *Adv. Phys.* **25**, 343 (1976); J. S. Langer and A. J. Schwartz, *Phys. Rev. A* **21**, 948 (1980); R. J. Lovett, *J. Phys. Chem.* **84**, 1483 (1980); *J. Chem. Phys.* **81**, 6191 (1984); J. W. Cahn and J. E. Hilliard, *ibid.* **28**, 258 (1958).
7. J. P. Franck and H. G. Hertz, *Z. Phys.* **143**, 559 (1956).
8. J. L. Katz and B. J. Ostermeier, *J. Chem. Phys.* **47**, 478 (1967).
9. J. L. Katz, *ibid.* **52**, 4733 (1970).
10. ———, C. J. Scoppa II, N. G. Kumar, P. Mirabel, *ibid.* **62**, 448 (1975).
11. P. Mirabel, C. J. Scoppa II, T. L. Virkler, *ibid.* **65**, 382 (1976).
12. R. H. Heist and H. Reiss, *ibid.* **59**, 665 (1973).
13. A. Kacker and R. H. Heist, *ibid.* **82**, 2734 (1985).
14. C. Becker, H. Reiss, R. H. Heist, *ibid.* **68**, 3585 (1978).
15. C. Becker, *ibid.* **72**, 4529 (1980).
16. M. A. Chowdhury, *ibid.* **80**, 4569 (1984).
17. J. L. Schmitt, *Rev. Sci. Instrum.* **52**, 1749 (1981).
18. H. Flood, *Z. Phys. Chem. A* **170**, 286 (1934); H. Reiss, *J. Chem. Phys.* **18**, 840 (1950).
19. G. Wilemski, *J. Chem. Phys.* **62**, 3763 (1975); D. Stauffer, *J. Aerosol Sci.* **7**, 319 (1976); J. P. Garnier, P. Mirabel, B. Migault, *Chem. Phys. Lett.* **115**, 101 (1985); R. G. Renninger, F. C. Hiller, R. C. Bone, *J. Chem. Phys.* **75**, 1584 (1981); G. Wilemski, *ibid.* **80**, 1370 (1984); P. Mirabel and H. Reiss, *Langmuir* **3**, 228 (1987).
20. H. Reiss, H. Rabeony, M. S. El-Shall, A. Bahta, *J. Chem. Phys.* **87**, 1315 (1987).
21. H. Reiss and P. Mirabel, *J. Phys. Chem.* **91**, 1 (1987).
22. H. Crane and J. Halpern, *Phys. Rev.* **56**, 232 (1939).
23. L. B. Allard and J. L. Kassner, Jr., *J. Colloid Interface Sci.* **30**, 81 (1969).
24. G. J. Doyle, *J. Chem. Phys.* **35**, 795 (1961); P. Mirabel and J. L. Katz, *ibid.* **60**, 1138 (1974); R. H. Heist and H. Reiss, *ibid.* **61**, 573 (1974); W. J. Shugard, R. H. Heist, H. Reiss, *ibid.*, p. 5298; W. J. Shugard and H. Reiss, *ibid.* **65**, 2827 (1976); P. Mirabel and J. L. Clavelin, *ibid.* **68**, 5020 (1978).
25. E. J. Hart, K. H. Schmidt, K. N. Vasudevan, *Science* **180**, 1064 (1973); D. C. Marvin and H. Reiss, *J. Chem. Phys.* **69**, 1897 (1978); P. Mirabel and J. L. Clavelin, *ibid.* **70**, 2048 (1979); *ibid.*, p. 5767.
26. B. Cordier, P. Papon, J. Leblond, *J. Chem. Phys.* **74**, 3353 (1981); J. L. Katz, J. G. Ruggiero, Jr., R. Partch, D. Warren, F. H. Ebetino, *ibid.* **79**, 2763 (1983); S. P. Buxbaum, Z. Hag, J. L. Katz, R. Partch, *ibid.* **85**, 5207 (1986).
27. J. L. Katz, F. C. Wen, T. McLaughlin, R. J. Reusch, R. Partch, *Science* **196**, 1203 (1977); J. L. Katz, T. McLaughlin, F. C. Wen, *J. Chem. Phys.* **75**, 1459 (1981); F. C. Wen, T. McLaughlin, J. L. Katz, *Phys. Rev. A* **26**, 2235 (1982).
28. A. W. Gertler, J. O. Berg, M. A. El-Sayed, *Chem. Phys. Lett.* **57**, 343 (1978).
29. M. A. Chowdhury, H. Reiss, D. R. Squire, V. Stannett, *Macromolecules* **17**, 1436 (1984).
30. H. Reiss and M. A. Chowdhury, *J. Phys. Chem.* **88**, 6667 (1984).
31. H. Reiss, in *Advances in Chemical Reaction Dynamics*, P. M. Rentzepis and C. Capellos, Eds. (Reidel, Dordrecht, Netherlands, 1985), pp. 71–113.
32. P. J. Flory, *J. Am. Chem. Soc.* **62**, 1561 (1940).
33. J. B. Harkness, G. B. Kistiakowsky, W. H. Mears, *J. Chem. Phys.* **5**, 682 (1937); A. C. Cuthbertson, G. Gee, E. K. Rideal, *Nature (London)* **140**, 889 (1937).
34. C. Walling, E. R. Briggs, F. R. Mayo, *J. Am. Chem. Soc.* **68**, 1145 (1946).
35. R. H. Boundy and R. F. Boyer, *Styrene, Its Polymers, Copolymers and Derivatives* (Reinhold, New York, 1952), pp. 221 and 216 (table 7-11); A. Lebovits and W. C. Teach, *J. Polym. Sci.* **47**, 527 (1961).
36. M. S. El-Shall, A. Bahta, H. Rabeony, H. Reiss, *J. Chem. Phys.* **87**, 1329 (1987).
37. H. Rabeony and H. Reiss, *Macromolecules*, in press.
38. J. L. Schmitt, personal communication. Schmitt has been conducting measurements on the steady-state distribution of polymeric radicals in styrene vapor, using a high-precision expansion cloud chamber. Preliminary results provide definitive evidence of the self-initiated polymerization of styrene in the gas phase. The results also indicate that a time of the order of 10 minutes is required to set up the steady-state distribution after the larger polymers are removed by adiabatic expansion and nucleation. Substitution of preliminary data into Eq. 5 suggests that the thermal rate of generation of initiating free radicals is on the order of 1.0 cm^{-3} sec^{-1}.
39. M. S. El-Shall, H. Rabeony, A. Bahta, H. Reiss, unpublished results.
40. R. Simha and H. Branson, *J. Chem. Phys.* **12**, 253 (1944).
41. M. S. El-Shall, H. Rabeony, H. Reiss, unpublished results.
42. S. J. Landon, P. M. Shulman, G. L. Geoffroy, *J. Am. Chem. Soc.* **107**, 6739 (1985).
43. F. Williams, K. Hayashi, K. Ueno, K. Hayashi, S. Okamura, *Trans. Faraday Soc.* **63**, 1501 (1967).
44. F. Williams, in *Fundamental Processes in Radiation Chemistry*, P. Ausloos, Ed. (Wiley, New York, 1968), pp. 515–598.
45. L. Onsager, *J. Chem. Phys.* **2**, 433 (1934).
46. V. T. Stannett, *Br. Polym. J.* **1981**, 93 (September 1981).
47. A. Deffieux, V. Stannett, A. Wang, J. A. Young, D. R. Squire, *Polymer* **24**, 1469 (1983).

48. This work was supported by NSF grant DMR-84-21383. I am indebted to J. L. Schmitt for communicating data, in advance of publication, on the gas-phase polymerization of styrene.